A PARTICLE SWARM OPTIMIZATION BASED FUZZY FLCPI-PSO CONTROLLER FOR QUADCOPTER SYSTEM

Mohammed Baba[1,*], Fateh Bounaama[2], Sid Bennaceur[3], Aissa Benhammou[1], Mohammed Amine Soumeur[1]

[1]Laboratory of Smart Grids and Renewable Energies (SRGE), University Tahri Mohammed Bechar, Bechar, Algeria
[2]Laboratory of Energy in Arid Zones (ENERGARID), University Tahri Mohammed Bechar, Bechar, Algeria
[3]Laboratory of Renewable Energies and their Applications in Saharan areas (LDREAS), University Tahri Mohammed Bechar, Bechar, Algeria

*E-mail of corresponding author: baba.mouhamed@univ-bechar.dz

Mohammed Baba 0000-0002-8644-3253,
Fateh Bounaama 0000-0001-7230-5792,
Said Benaceur 0000-0003-4911-8694,
Aissa Benhammou 0000-0003-3313-2571,
Mohammed Amine Soumeur 0000-0001-9303-4880

Resume

The quadcopter persist as important roles across diverse applications, and the enhancement of their control efficacy has been the subject of extensive research.
In this work, the authors proposed optimal Proportional Integral (PI) controller based Fuzzy Logic Control (FLC) for the roll, pitch, altitude, and yaw motions of the quadcopter system.
The proposed technique uses the Particle Swarm Optimization (PSO) algorithm to tune the parameters of the FLC and enhance the quadcopter performance. The simulation results show that the proposed technique achieves smoothness of control and significant improvement over classical techniques, as the rise time and the settling time are reduced by 61% and 66%, respectively. These times are important for stabilizing the system's response speed and avoiding overshooting or oscillating. This indicates that the FLCPI-PSO can achieve the desired roll and altitude angles more rapidly and effectively.

Available online: https://doi.org/10.26552/com.C.2024.027

Article info

Received 21 September 2023
Accepted 18 March 2024
Online 4 April 2024

Keywords:

quadcopter model
fuzzy logic controller
optimization
FLCPI-PSO

ISSN 1335-4205 (print version)
ISSN 2585-7878 (online version)

1 Introduction

Quadcopter drones, as autonomous aerial vehicles, have garnered significant attention from both researchers and manufacturers due to their versatility in exploration and study. Their compact size and unique capabilities for spatial monitoring and infrastructure inspection have spurred the evolution of such systems. Among the various drone configurations, Vertical Take-Off and Landing (VTOL) models are particularly noteworthy for their lightweight motors and efficient propeller arrangements that eliminate the need for a tail rotor, thus simplifying the control mechanism [1].

The topology of quadcopters typically involves front and rear motors of the same diameter rotating in opposite directions to their diametric counterparts, which negates gyroscopic effects and facilitates stable flight [2-4]. The study of the input forces influence on output coordinates reveals a strongly coupled dynamic system [5].

Advancements in control methods have been applied across diverse fields, including electric cars [6-7], power electronics [8], and hybrid electric systems [9-10]. To meet the increasing performance demands of quadcopters, enhancements in controller design have been implemented, such as Feedback Linearity (FBL) [11-12], Sliding Mode Control (SMC) [13-14], and backstepping methods [15-16]. Comparative analyses of various controllers, including Proportional Integral Derivative (PID), linear quadratic regulator (LQR), and modified PID with LQR control, are well-documented [17-18].

Fuzzy logic models, specifically the Takagi-Sugeno (TS) and Mamdani types, are the two fundamental and distinct approaches in intelligent control systems that have been integrated into electrical systems alongside Neural Networks (NN) [4, 19-21], Neuro-

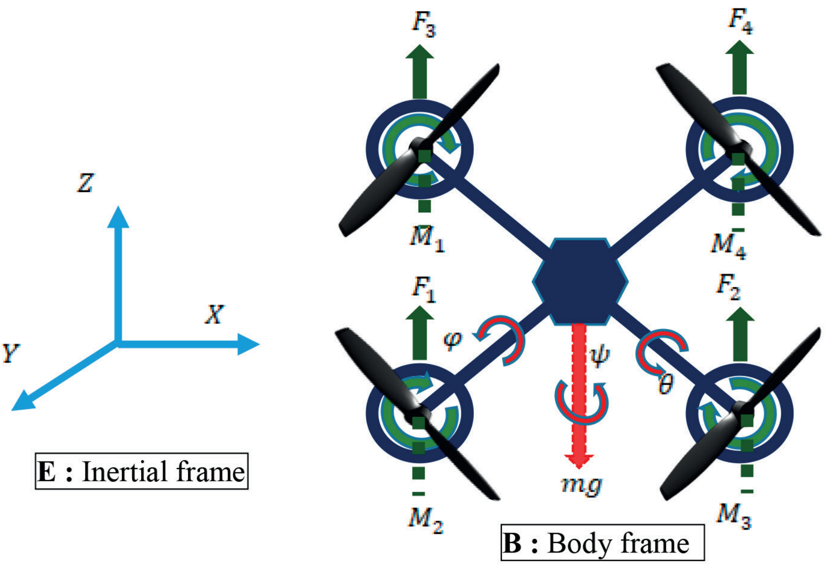

Figure 1 *The structure of quadcopter*

Fuzzy methodology [22-23], and Iterative Learning Control (ILC) [24-25]. These intelligent control methods are adept at managing unpredictable, non-linear, time-varying, and non-deterministic systems [26]. Fuzzy logic, in particular, is capable of handling the disturbances and noises (rotor vibrations) that quadrotors frequently encounter [27].

It has been noted that fuzzy control necessitates precise technology for selecting input constants [28]. The modular architecture of the fuzzy controller facilitates its integration with various optimizers to circumvent limitations.

In this paper, the mathematical model was developed using the Newton-Euler method to control altitude Z, roll (φ), pitch (θ), and yaw (ϕ) angles.

To accurately and steadily navigate the quadcopter, a FLC and an optimized fuzzy PID controller (FLCPI-PSO) are utilized for the control component, representing the core contribution of this work. The novelty of this paper lies in evaluating the quadcopter's behavior and performance through the optimization of a basic FLC with a swarm technique. This proposed control technique endows the quadcopter with acceptable response times, thereby enhancing its behavior—a facet not previously explored in other studies.

The remainder of this research paper is organized as follows: Section 1 presents the mathematical model, Section 2 discusses the control strategy, Section 3 contains the simulation results and discussion, and the paper concludes with the conclusions and future perspectives of this study.

2 Mathematical model

A quadcopter is an aerial vehicle equipped with four rotors that enable 360-degree maneuverability. To accurately describe the system dynamics, it is essential to understand the concept of six degrees of freedom, which represents the location and orientation of the quadcopter in three-dimensional (3-D) space. The six degrees of freedom are defined using two reference frames as illustrated in the quadcopter structure shown in Figure 1:

1. The inertial or earth frame, a fixed coordinate system represented by the x, y, and z coordinates, corresponding to the cardinal directions of north, east, and down. This frame serves as the initial reference point.
2. The body frame, a movable coordinate system centered around the quadcopter's center of gravity, described by the angles (φ), (θ), and (ϕ) in relation to the inertial frame.

Given that the quadcopter has four inputs and six outputs, it is classified as an underactuated nonlinear system. To facilitate the controller design, sensible assumptions are made to model the system dynamics of the quadcopter effectively [29].

2.1 Kinematic model

To derive a model for the quadcopter motions it is necessary to examine different moments and forces acting on the quadcopter.

We assume $\xi = [XYZ]$ to be the position and the linear velocity $V = [uvw]$, and let $\eta = [\phi\theta\phi]$ to be rotational angles and angular velocity is $\omega = [pqr]$.

Using the Newton-Euler equations and the information proaccessed in Equation (1), one can determine the forces and moments acting on the quadcopter [30]:

$$\begin{bmatrix} F \\ \tau \end{bmatrix} = \begin{bmatrix} mI_{3\times 3} & 0 \\ 0 & 1 \end{bmatrix} + \begin{bmatrix} \omega \times m\xi \\ \omega \times I\eta \end{bmatrix}, \tag{1}$$

where; F and τ represent the force and torque vector, respectively, generated by the four motors' rotation acting on the quadcopter, m is the mass of the quadcopter, $\dot{V}$ and $\dot{\omega}$ represent linear and angular acceleration vector, respectively, all with respect to the body frame, and $I_{3\times 3}$ represents the moments of inertia matrix and is given as:

$$I=\begin{bmatrix} I_{xx} & 0 & 0 \\ 0 & I_{yy} & 0 \\ 0 & 0 & I_{zz} \end{bmatrix}. \tag{2}$$

Typically, the angular positions and velocities above are in a different frame, so we need some kind of transformation matrix to go from one reference frame to the other. The rotation R and transfer T matrices, respectively, are used to derive the translational and rotational kinematic equations [31]. Equations (3) and (4), respectively, proaccesseded the expressions for the rotation R and transfer T matrices.

$$R=\begin{bmatrix} c\phi c\theta & c\phi s\theta s\varphi - s\phi c\varphi & c\phi s\theta c\varphi + s\phi c\varphi \\ s\phi c\theta & s\phi s\theta s\varphi - c\phi c\varphi & s\phi s\theta c\varphi - c\phi s\varphi \\ -s\theta & c\theta s\varphi & c\theta c\varphi \end{bmatrix}, \tag{3}$$

$$T=\begin{bmatrix} 1 & t\theta s\varphi & t\theta c\varphi \\ 0 & c\varphi & -s\varphi \\ 0 & s\varphi / c\theta & c\varphi / c\theta \end{bmatrix}, \tag{4}$$

where, $c\theta = \cos\theta, s\theta = \sin\theta,$ and $t\theta = \tan\theta$.

- The translational kinematics:

$$\dot{\xi} = RV, \tag{5}$$

where $\dot{\xi}$ are linear velocity vector with respect to the earth frame E and V is the linear velocity vector with respect to body frame B.

- The rotational kinematics:

$$\dot{\omega} = T\dot{\eta}, \tag{6}$$

where $\dot{\omega}$ is the angular velocity vector with respect to the earth frame E and $\dot{\eta}$ the angular velocity vector with respect to body frame B.

2.2 Dynamic model

The translational dynamic equations of the quadcopter are given as follows in accordance with the Euler's first rule of motion for rigid body dynamics:

$$m\begin{bmatrix} \ddot{X} \\ \ddot{Y} \\ \ddot{Z} \end{bmatrix} = \begin{bmatrix} 0 \\ 0 \\ -mg \end{bmatrix} + RU_1, \tag{7}$$

where g is the gravity acceleration and U_1 is the total thrust generated by the four rotors:

$$U_1 = \sum_{i=1}^{4} F_i = b\sum_{i=1}^{4} \Omega_i^2, \tag{8}$$

where $b[N\,s^2]$ is the thrust coefficient and $\Omega\left[\frac{rad}{\sec}\right]$ is the angular velocity of the rotor i.

From Equation (1) and the Newton-Euler formalism, we obtain the rotational motion equations:

$$I\ddot{\eta} = \tau - \dot{\eta} \times I\dot{\eta} - \dot{\eta} \times [0 \;\; 0 \;\; I_r\Omega_r], \tag{9}$$

where I is an inertia matrix of the quadcopter, I_r is the inertia of the rotors, Ω_r is the relative speed and τ is the moment acting on the quadcopter in the body frame.

$$\Omega_r = (-\Omega_1 - \Omega_3 + \Omega_2 + \Omega_4), \tag{10}$$

$$\tau = \begin{bmatrix} U_2 \\ U_3 \\ U_4 \end{bmatrix} = \begin{bmatrix} bl(\Omega_4^2 - \Omega_2^2) \\ bl(\Omega_3^2 - \Omega_1^2) \\ dbl(\Omega_4^2 - \Omega_2^2 - \Omega_3^2 + \Omega_4^2) \end{bmatrix}, \tag{11}$$

where d $[N\,m\,s^2]$ is the drag coefficient and l [m] is the distance between the center of the quadcopter and the center of a propeller.

From Equation (7) and Equation (9), the equations motion of the quadcopter are given as follows:

$$\ddot{X} = (\sin\phi\sin\varphi + \cos\phi\sin\theta\cos\varphi)\frac{U_1}{m}, \tag{12}$$

$$\ddot{Y} = (-\cos\phi\sin\varphi + \sin\phi\sin\theta\cos\varphi)\frac{1}{m}U_1, \tag{13}$$

$$\ddot{Z} = -g + \frac{1}{m}(\cos\theta\cos\varphi)U_1, \tag{14}$$

$$\ddot{\varphi} = \frac{\dot{\theta}\dot{\phi}(I_{yy} - I_{zz})}{I_{xx}} - \frac{J_r}{I_{xx}}\Omega_r\dot{\theta} + \frac{U_2}{I_{xx}}, \tag{15}$$

$$\ddot{\theta} = \frac{\dot{\varphi}\dot{\phi}(I_{zz} - I_{xx})}{I_{yy}} + \frac{J_r}{I_{yy}}\Omega_r\varphi + \frac{U_3}{I_{yy}}, \tag{16}$$

$$\ddot{\phi} = \frac{\dot{\theta}\dot{\varphi}(I_{xx} - I_{yy})}{I_{zz}} + \frac{U_4}{I_{zz}}. \tag{17}$$

3 Control strategy

3.1 Fuzzy logic controller (FLC)

The FLC is the consequence of Zadeh's fuzzy set notion in 1965. Fuzzy set theory was graded from non membership to membership. Thus, the boundaries of fuzzy sets might be unclear and ambiguous, making them suitable for approximation systems. If correct mathematical formulations are problematic, the FLC is the best accessible solution. Other FLC benefits include:

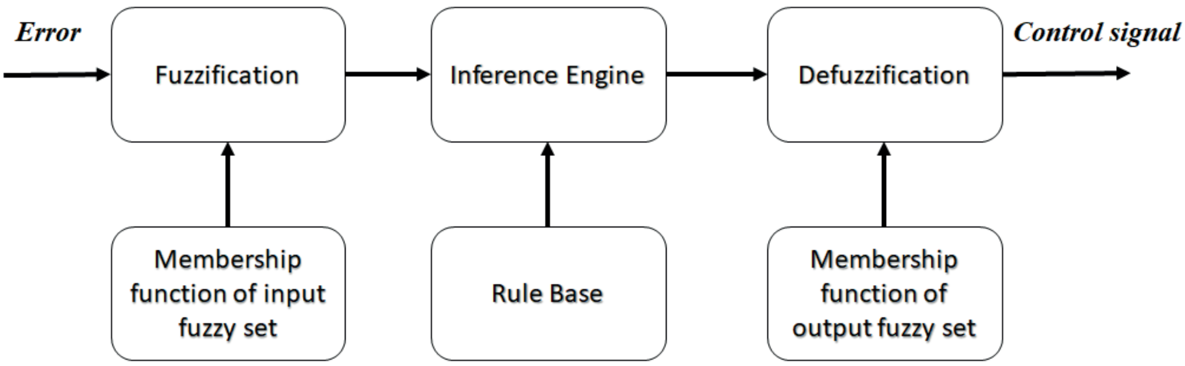

Figure 2 *The structure of the Fuzzy Logic Control*

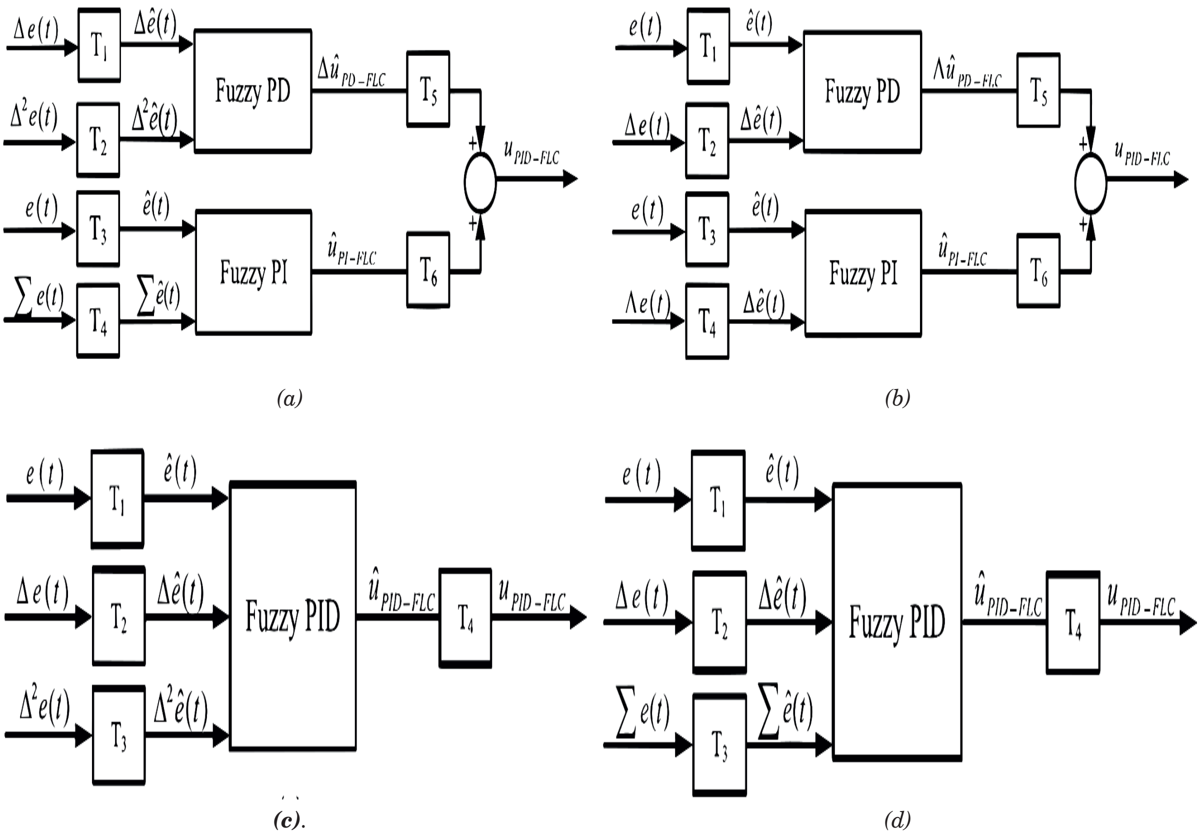

Figure 3 *Common PID-type fuzzy logic controllers [28]*

1. It may seek to proaccessed less precise outcomes.
2. There is no requirement for rapid processors.
3. It does not take as much data storage in the formula of rule and membership function MF as compared to typical controllers.

The structure of the FLC is given in Figure 2.

The direct action fuzzy controller structure is simply referred to as PID-type fuzzy controller or PID-FLC. However, the term fuzzy PID controller (or FLCPI) refers to the so-called gain scheduling-type PID controllers, which are not covered in this work. In these controllers, fuzzy logic is employed to generate the necessary KP, KI, and KD gains for the linear PID controller. The amount of inputs to the fuzzy PID controllers determines how they are often categorized. The most prevalent fuzzy control architectures, in which a nonlinear PID-like performance is anticipated from the controller, are often two- and three-input fuzzy controllers. Figure 3 shows a few of the most widely utilized structures. It should be noted that the fuzzy controllers' input/output variables are normalized to fall between [1-1]. As a result, the first two structures (see Figure 3.a and 3.b) need the appropriate selection of six scaling factors, while the last two structures (see Figure 3.c and 3.d) require the proper selection of four scaling factors [28].

Throughout this study, a different structure is used; it is shown in Figure 4. The proaccesseded structure has one single two-input fuzzy controller, which makes

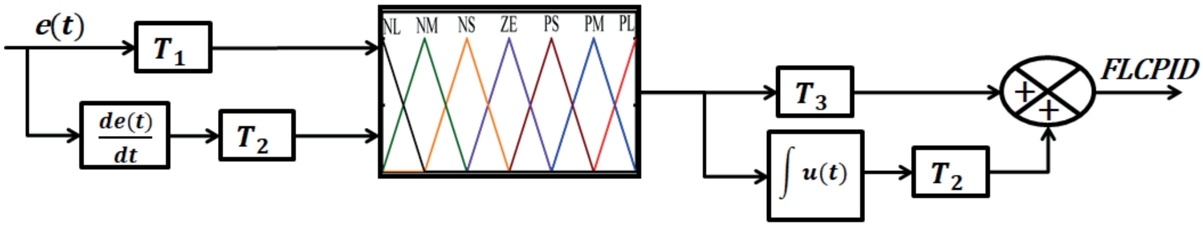

Figure 4 *Alternative fuzzy PID controller*

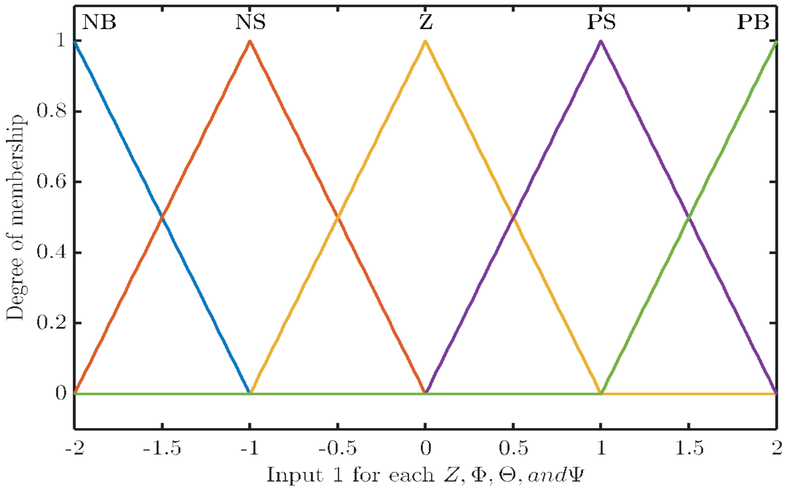

Figure 5 *The MF for the input variable error of altitude and three angle roll, pitch, yaw*

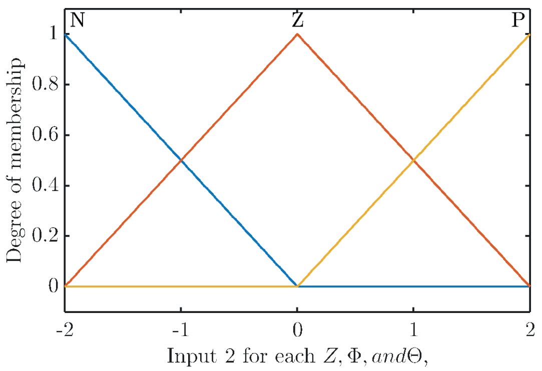

Figure 6 *The MF for the input variable (de) derivative error for roll and pitch angle and altitude*

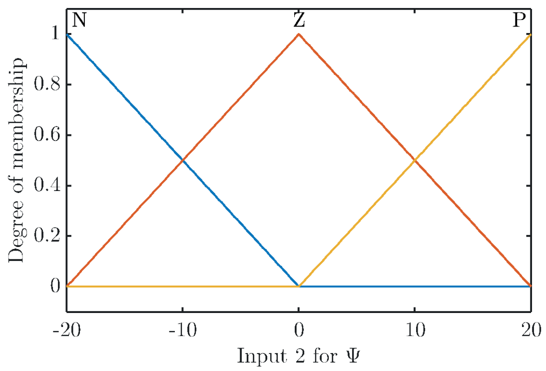

Figure 7 *The MF for the input variable (de) derivative error for the yaw angle*

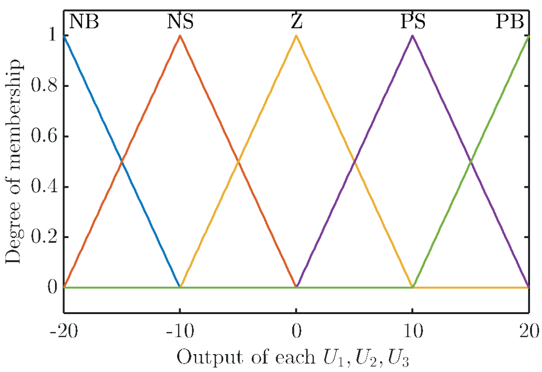

Figure 8 *The MF for the output variable* (*U*1, *U*2, *U*3)

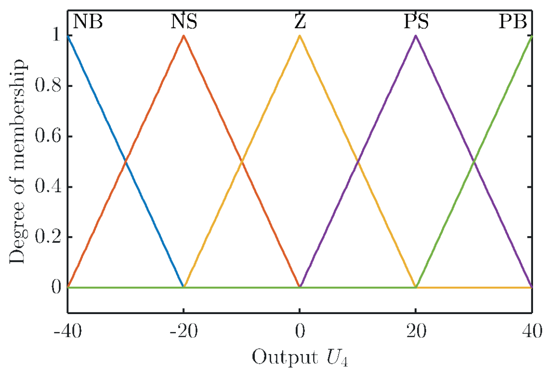

Figure 9 *The MF for the output variable* (*U*4)

Table 1 The rules base for the four fuzzy logic controllers (altitude, roll, pitch, and yaw Controllers)

e / de	NB	NM	Z	PM	PB
N	NB	NM	NM	Z	PM
Z	NB	NM	Z	PM	PB
P	NM	Z	PM	PM	PB

it computationally more efficient for the real-time implementation when compared to that in Figure 3. In comparison to three-input architectures, the fuzzy controller only needs two inputs, hence fewer rule bases need to be constructed.

This study is thus limited to fuzzy controllers of the Mamdani-Type.

3.1.1 Fuzzification

The total control system for the quadcopter with the Fuzzy PID controllers for the four fundamental quadcopter movements thrust, roll, pitch, and yaw is depicted in Figure 4. The triangle membership function has been utilised for each of the inputs and the outputs and for all of the controllers. The inputs, errors are defined by five membership functions MF: NB (negative big), NS (negative small), Z (zero), PS (positive small), and PB (positive big), and the error derivative is defined by three membership functions: P(positive), Z(zero), N(negative). On the other hand, each of the outputs is specified by five membership functions: NB (negative big), NS (negative small), Z (zero), PS (positive small), and PB (positive big). The range of the fuzzy set for the error input for all controllers (altitude, roll, pitch, and yaw) has been chosen as [-2, 2], and for the error derivative for (altitude, roll, and pitch controllers) as [-4, 4], and [-20 20] for the error derivative of yaw controller. Figures 5 to 7 show the membership functions for the inputs.

The range for the outputs fuzzy set has been chosen as follows:

- [-20, 20] for $U1$, $U2$, $U3$, and as indicated in Figure 8,
- [-40, 40] for $U4$ and as indicated in Figure 9.

3.1.2 Rules base

After specifying the inputs and outputs for each fuzzy controller, we established the rules base.

The fuzzy rules suggest that "if error is E_i and error change is DE_i, then production is U_i". The fuzzy inference procedure of the controller parameters leverages the Mamdani approach. Five variables refer to errors, and three error changes are added to the 15 rules.

If the change in error is NB and the error is NB, then the outcome will be NB, as well. The response signal is fed back and subtracted from the set value to generate the error signal, and then the change in error is determined after the subtraction. Those two signals are sent as inputs to the controller. Table 1 shows the rules base for each controller.

3.1.3 Defuzzification

Fuzzification's counterpart is known as defuzzification. The fuzzy set generated by the FLC inference engine must be transformed to actual value (crisp output) in line with the real-world requirements. Defuzzification implies the weighted average approach. The weighted average strategy becomes the illustrating point, which is the centre of the region generated by the curve and abscissa of the fuzzy membership function. Theoretically, the centre of gravity of a set of sites within the output scope must be computed [32].

3.2 Particle swarm optimization algorithm

Finding the best solutions involves using a variety of optimisation techniques. Evolutionary and meta-heuristic approaches work best when employed for route planning.

Numerous evolutionary techniques have been demonstrated to be useless when route planning procedures have an excessively wide search area. The exciting findings from this vast area of study may help the meta-heuristic systems to overcome these limitations.

The population-based stochastic optimisation method, known as the particle swarm optimisation (PSO), is very similar to evolutionary computing methods like genetic algorithms (GA). The PSO has been effectively used in several research and application domains over the last few years because it produces better results more quickly with fewer parameters to alter.

The PSO uses particles to represent possible solutions, which follow the current optimal particles as they move around the problem space. According to their prior behaviours, particles move around the search space at velocities that are dynamically changed.

The system starts out with a population of random solutions and updates generations in an effort to find the best option. The location of a point $X_i = (x_{i,1}, x_{i,2}, \ldots, x_{i,d}) \in S$ in an S-dimensional space serves as the representation of the i-th particle. Each particle keeps track of three values during the process: its best position in previous cycles; its present position,

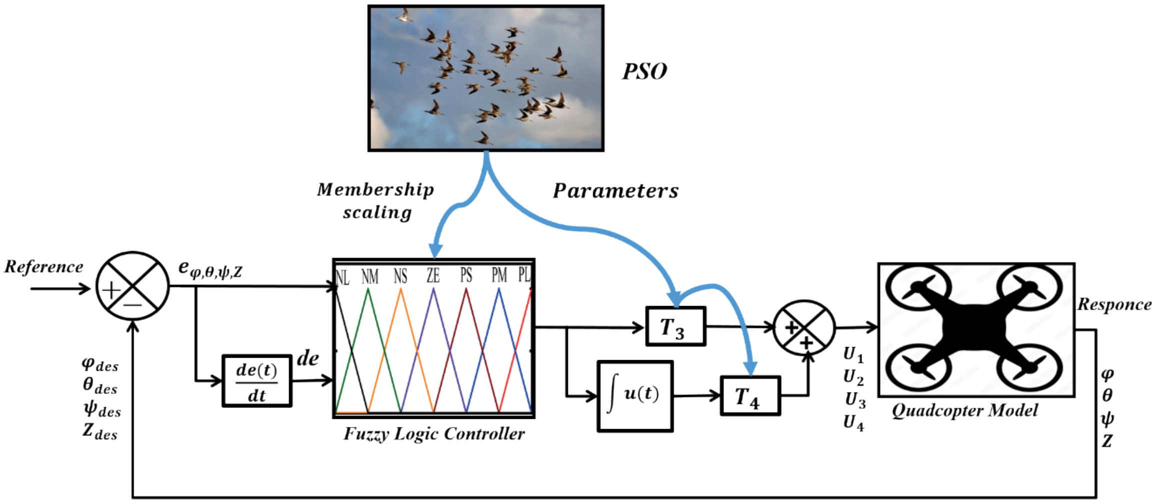

Figure 10 *Structure of FLCPI-PSO controller*

X_i. $pbest_i = (pbest_{i,1}, pbest_{i,2}, pbest_{i,3}, \ldots, pbest_{i,d}) \in S$; and the speed of its flight $V_i = (v_{i,1}, v_{i,2}, v_{i,3}, \ldots, v_{i,d})$. To catch up to the leading particle, each particle modifies its location and velocity, such as:

$$X_i(t+1) = X_i + (t) + V_i(t+1), \tag{18}$$

$$V_i(t+1) = V_i(t) + c_1 r_{i,1}(t)(pbest_i(t) - \\ - X_i(t)) + c_2 r_{i,2}(t)(gbest(t) - X_i(t)). \tag{19}$$

The best track value for each particle in iteration t is denoted by $pbest_i$, and the best position of the entire swarm is denoted by gbest. The cognitive and social parameters are denoted, respectively, by c_1 and c_2, two positive constants (acceleration coefficients), and $r_{i,1}$ and $r_{i,2}$, two random functions in the [0, 1] range.

The following is a summary of an approach to determine the optimal placement vector for the PSO with n Agents:

1. Using the random numbers, the initial positioning vector X [n] and velocity vector V [n] are created.
2. Using Equation (1), agent i's velocity vector $V_i(t+1)$ is determined.
3. Equation (2) is used to determine agent i's new positioning vector, $X_i(t)$.
4. The positioningVector X_i is set to $pbest_i$ if $F(X(t))$ is superior than $F(pbest_i)$. The positioning vector $gbest$ is set to $pbest_i$ if $F(gbest_j)$ is superior than $F(gbest)$.
5. When the required number of iterations has been reached, stop. If not, go to step 2.

The first design is a Mamdani-type two-input PID-type fuzzy controller, as shown in Figures 2 and 3. The membership functions in the first level of tuning are uniformly distributed, and the meta-heuristic techniques must be used to tune the scaling factors and parameters T_1, T_2, T_3, and T_4. PSO is employed at this point to identify the ideal scaling factors and parameters T_1, T_2, T_3, and T_4. The optimisation approach is used to reduce many common time domain objective functions, including the integral time absolute of error (ITAE).

The structure of the FLCPI-PSO controller is depicted in Figure 10.

4 Simulation results and discussion

In the design process and simulation studies, a 1-step unit is applied to each height and roll, pitch, and yaw angle concurrently at t = 0 s. The simulation is carried out with Matlab 2017 programme and Simulink Toolbox. The simulation was done on an SGRE laboratory computer with a Intel(R) Core(TM) i7-5820K, 3.30 GHz, 64 GB of RAM, and Windows 10.

The MATLAB Simulink is used to mimic two type of controllers, FLCPI and FLCPI-PSO. These controllers were employed to control the quadcopter systems. The FLCPI with a one-of-a-kind configuration that is adjusted manually and FLCPI-PSO that is tuned via the PSO method Integral Time Absolute Error (ITAE) is used as a criterion for the control performance assessment as in Equation (20).

$$ITAE = \int t|e(t)|dt. \tag{20}$$

Figure 11 displays the objective function of PSO algorithm.

As a result, the tuned scaling factors and parameters of four controllers are presented in Table 2.

The quadcopter system response, after an occurrence of step-unit changes is depicted in Figures 12 to 15. The responses quadcopter system characteristics are summarized in Table 3.

The control signals (U_1 through U_4), which represent the desired thrust force and torques, are shown in Figures 16 to 19.

The results presented in Figures 12-15 and Table 3 illustrate the comparative performance of the FLC

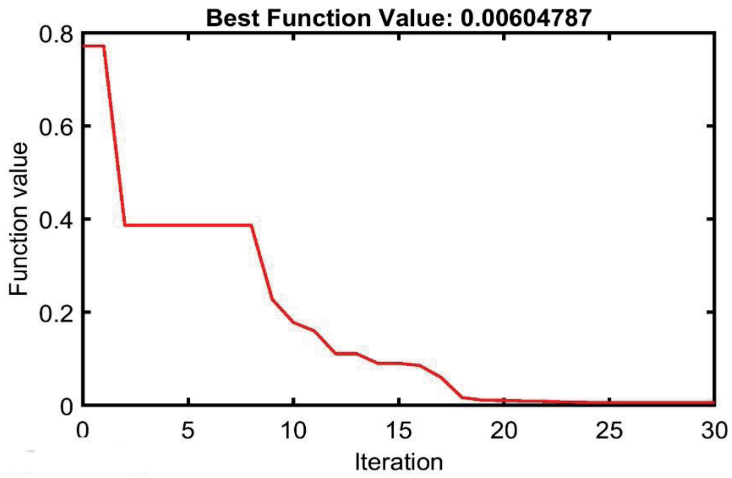

Figure 11 *Objective function of PSO algorithm*

Table 2 *Scaling factors and parameters optimized by the PSO*

	Scaling factors		Parameters	
	T1	T2	T3	T4
Altitude	6.1868	55.9443	88.8980	40.2961
Roll	100.0000	99.0577	23.0000	0.2000
Pitch	1.0000	99.1495	77.0602	1.0000
Yaw	9.2101	45.8878	9.0000	0.2300

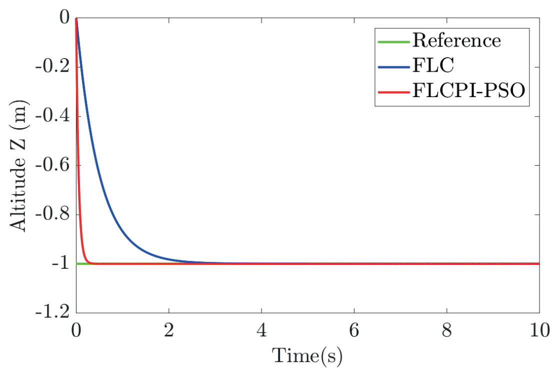

Figure 12 *The altitude signal response for the FLC and the FLCPI-PSO controllers*

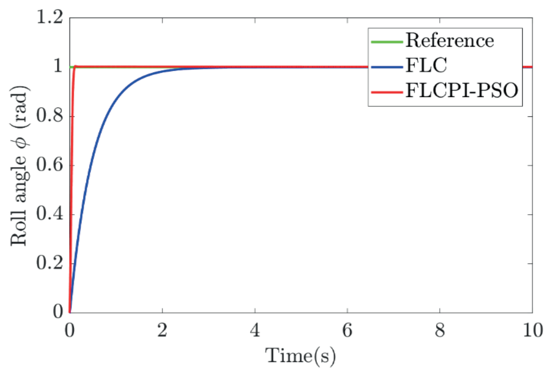

Figure 13 *The roll signal response for the FLC and the FLCPI-PSO controllers*

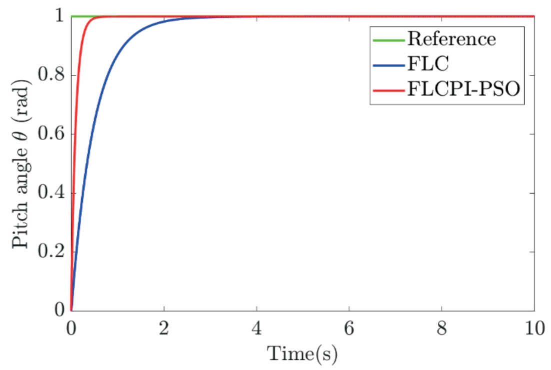

Figure 14 *The pitch signal response for the FLC and the FLCPI-PSO controllers*

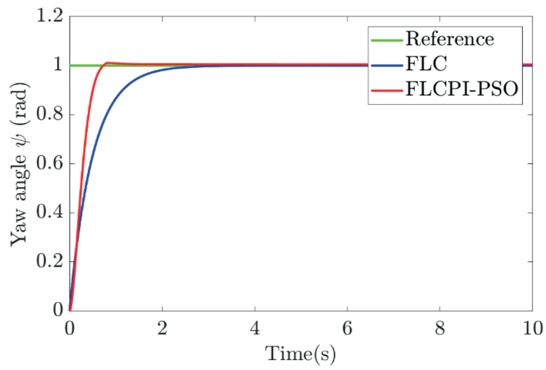

Figure 15 *The yaw signal response for the FLC and the FLCPI-PSO controllers*

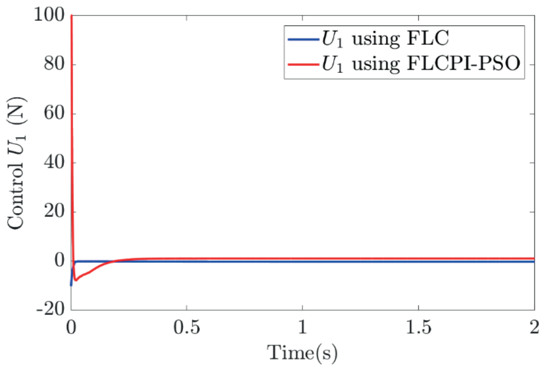

Figure 16 *Control signal U_1 for the FLC and the FLCPI-PSO controllers*

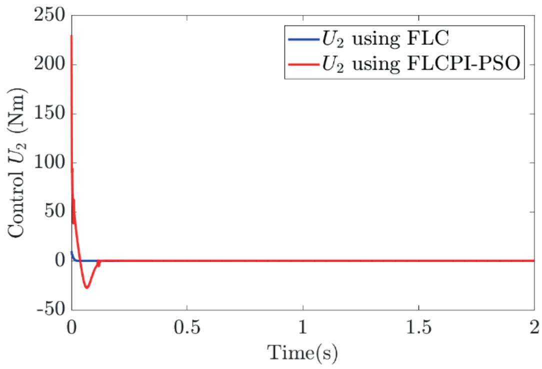

Figure 17 *Control signal U_2 for the FLC and the FLCPI-PSO controllers*

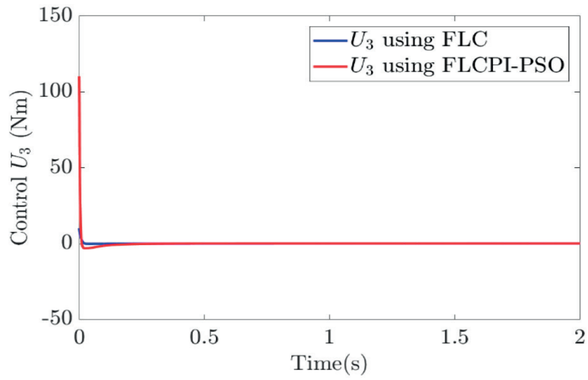

Figure 18 *Control signal U_3 for the FLC and the FLCPI-PSO controllers*

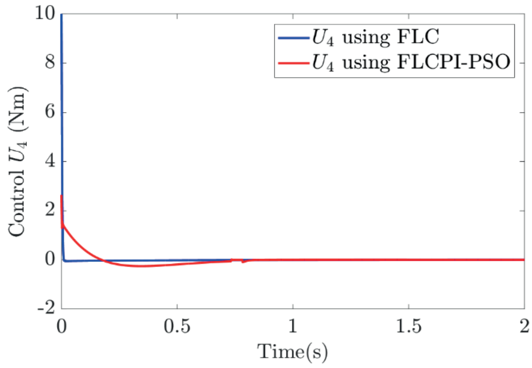

Figure 19 *Control signal U_4 for the FLC and the FLCPI-PSO controllers*

Table 3 *Responses to a step function with different control*

	Controllers							
	Altitude		Roll		Pitch		Yaw	
Performances	FLC	FLCPI-PSO	FLC	FLCPI-PSO	FLC	FLCPI-PSO	FLC	FLCPI-PSO
RiseTime (s)	1.0839	0.1157	1.0869	0.0605	1.0801	0.2143	1.0924	0.4257
SettlingTime (s)	1.9395	0.2094	1.9429	0.0954	1.9334	0.3851	1.9492	0.6632
Overshoot (%)	0	1.9000	0	31.6100	0	0	0	64.1100

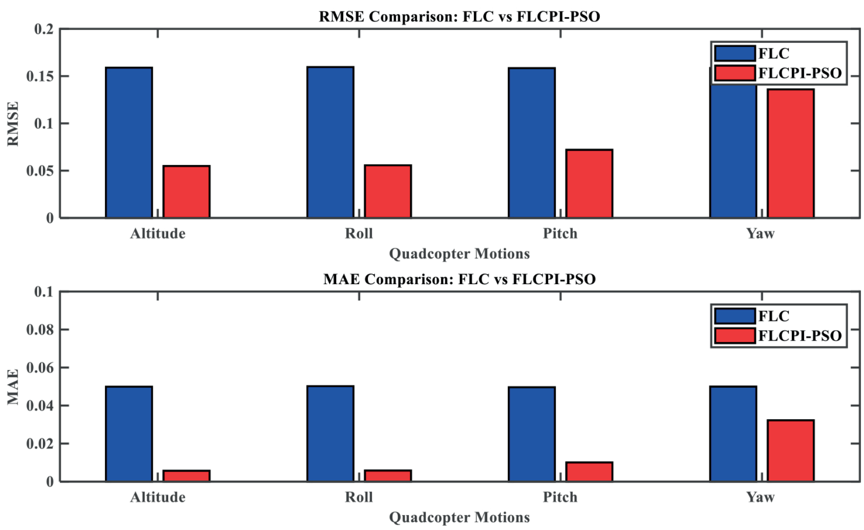

Figure 20 *Quadcopter control performance evaluation between the FLC and FLCPI-PSO*

and FLCPI -PSO controllers in managing the altitude, roll, pitch, and yaw of a quadcopter. It is evident that the FLCPI -PSO controller consistently outperforms the FLC controller across all parameters. The rise time for altitude, roll, pitch, and yaw is significantly reduced with FLCPI -PSO, indicating a quicker response to changes. Similarly, the settling time is also lower for all the inputs under the FLCPI -PSO control, denoting faster stabilization.

In terms of overshoot percentage, the FLC controller exhibits a 1.9000% overshoot in altitude and a substantial 31.6100% in roll but none in pitch and yaw. In contrast, the FLCPI -PSO controller effectively eliminates overshoot in all parameters except for yaw where it records a 64.1100% overshoot.

These findings underscore the enhanced efficiency and reliability of the FLCPI -PSO controller over its FLC counterpart in ensuring the rapid response times and minimal overshoots during quadcopter operation. The data suggests that the integrating PSO with fuzzy logic control (FLCPI) yields superior control precision and responsiveness.

Comparison of the quadcopter performance evaluation using the KPIs indexes between the FLC and FLCPI-PSO, is shown in Figure 20.

5 Conclusion

Based on the comparative analysis of the FLC and FLCPI-PSO for altitude, roll, pitch, and yaw in the quadcopter system, the FLCPI-PSO demonstrates superior performance in terms of faster rise time and settling time for altitude and roll control compared to the FLC. This indicates that the FLCPI-PSO can achieve the desired altitude and roll angles more efficiently and with quicker response times. The FLCPI-PSO offers advantages in terms of faster response times and shorter settling times for altitude and roll control in the quadcopter system. The trade-off is a potential increase in overshoot, particularly in the roll and yaw control. These findings highlight the importance of considering the specific requirements and trade-offs when selecting the appropriate controller for the quadcopter systems. Future research could focus on further optimizing the FLCPI-PSO to reduce the overshoot, while maintaining its performance advantages and its real-time implementation.

Acknowledgements

The authors thank the Algerian research direction DGRSDT, and the Smart Grids and Renewable Energies (SGRE) Laboratory, laboratory of Energy in Arid Zones (ENERGARID), and Laboratory of Renewable Energies and their Applications in Saharan areas (LDREAS), for supporting this research.

Conflicts of interest

The authors declare that they have no known competing financial interests or personal relationships that could have appeared to influence the work reported in this paper.

References

[1] PINES, D. J., BOHORQUEZ, F. Challenges facing future micro-air-vehicle development. *Journal of Aircraft* [online]. 2006, **43**(2), p. 290 -305. ISSN 1533-3868. Available from: https://doi.org/10.2514/1.4922

[2] HONG, M., BOUSBAINE, A., WU, M. H., POYI, G. T. Modelling and simulation of a quad-rotor helicopter. In: 6th IET International Conference on Power Electronics, Machines and Drives PEMD 2012: proceedings [online]. IEEE. 2012. eISBN 978-1-84919-616-1. Available from: https://doi.org/10.1049/cp.2012.0318

[3] LUPASHIN, S., SCHOLLIG, A., SHERBACK, M., D'ANDREA, R. A simple learning strategy for high-speed quadrocopter multi-flips. In: IEEE International Conference on Robotics and Automation: proceedings [online] [accessed 2023-09-21]. 2010, ISSN 1050-4729, p. 1642-1648. ISSN 1050-4729. Available from: https://doi.org/10.1109/ROBOT.2010.5509452

[4] MOHAMMED, B., SAID, B., FATEH, B. Feedforward neural network emulation of a PID continuous-time controller for quadcopter attitude digital control. *International Journal of Power Electronics and Drive Systems* [online]. 2023, **14**(2), p. 799-808 [accessed 2023-09-19]. ISSN 2088-8694. Available from: https://doi.org/10.11591/ijpeds.v14.i2.pp799-808

[5] ELAJRAMI, M., SATLA, Z., BENDINE, K. Drone control using the coupling of the PID controller and genetic algorithm. *Communications - Scientific Letters of the University of Zilina* [online]. 2021, **23**(3), p. C75-C82 [accessed 2024-01-18]. ISSN 1335-4205, eISSN 2585-7878. Available from: https://doi.org/10.26552/COM.C.2021.3.C75-C82

[6] BENHAMMOU, A., HARTANI, A.M., TEDJINI, H., REZK, H., AL-DHAIFALLAH, M. Improvement of autonomy, efficiency, and stress of fuel cell hybrid electric vehicle system using robust controller. *Sustainability* [online] 2023, **15**(7), 5657 [accessed 2024-01-18]. eISSN 2071-1050. Available from: https://doi.org/10.3390/SU15075657

[7] BENHAMMOU, A., TEDJINI, H., GUETTAF, Y., SOUMEUR, M. A., HARTANI, M. A., HAFSI, O., BENABDELKADER, A. Exploitation of vehicle's kinetic energy in power management of tow-wheel drive electric

vehicles based on ANFIS DTC-SVM comparative study. *International Journal of Hydrogen Energy* [online]. 2021, **46**(54), p. 27758-27769. ISSN 0360-3199. Available from: https://doi.org/10.1016/J.IJHYDENE.2021.06.023
[8] TOUFIK, T., TAHRI, U., BECHAR, M., ABDELKHALEK, O., AHMED, A., ABDELKADER, B., OTHMANE, A., AISSA, B., OUSSAMA, H. Dynamic voltage restorer using sliding mode controller: experimental studies Benhammou Aissa Dynamic voltage restorer using sliding mode controller: experimental studies. *International Journal of Applied Power Engineering* [online]. 2021, **10**(4), p. 337-346. ISSN 2252-8792. Available from: https://doi.org/10.11591/ijape.v10.i4.pp337-346
[9] BOUNAAMA, F., LAMMARI, K., DRAOUI, B., BOUNAAMA, F., LAMMARI, K., DRAOUI, B. Greenhouse air temperature control using fuzzy PD+I and neuro-fuzzy hybrid system controller. *International Journal on Numerical and Analytical Methods in Engineering (IRENA)* [online]. 2016, **4**(6), p. 172-178 [accessed 2024-01-18]. ISSN 2533-1736. Available from: https://doi.org/10.15866/IRENA.V4I6.12055
[10] AISSA, B., HAMZA, T., YACINE, G., AMINE, H. M. Impact of artificial intelligence in renewable energy management of hybrid systems. *Physical Sciences Forum* [online]. 2023, **6**(1), 5 [accessed 2024-01-18]. ISSN 2673-9984. Available from: https://doi.org/10.3390/PSF2023006005
[11] ALQAISI, W., BRAHMI, B., GHOMMAM, J., SAAD, M., NERGUIZIAN, V. Vision-based leader-follower approach for uncertain quadrotor dynamics using feedback linearisation sliding mode control. *International Journal of Modelling, Identification and Control* [online]. 2019, **33**(1), p. 9-19 [accessed 2023-09-21]. ISSN 1746-6180. Available from: https://doi.org/10.1504/IJMIC.2019.103980
[12] KUANTAMA, E., TARCA, I., TARCA, R. Feedback linearization LQR control for quadcopter position tracking. In: 2018 5th International Conference on Control, Decision and Information Technologies CoDIT 2018: proceedings [online] [accessed 2023-09-21]. IEEE: 2018. eISSN 2576-3555, 204-209. Available from: https://doi.org/10.1109/CODIT.2018.8394911
[13] CHIEW, T. H., LEE, H. E., LEE, Y. K., CHANG, K. M., ONG, J. J., EU, K. S. Second order sliding mode controller for altitude and yaw control of quadcopter. In: 2021 11th IEEE International Conference on Control System, Computing and Engineering ICCSCE 2021: proceedings [online]. IEEE. 2021. eISBN 978-1-6654-1281-0, p. 97-102. Available from: https://doi.org/10.1109/ICCSCE52189.2021.9530850
[14] SURAJ, S. K., GEORGE, V. I., THIRUNAVUKKARASU, I., VALSA PAUL, T. Design and simulation of a sliding mode-based control design for a quadrotor UAV. *Lecture Notes in Electrical Engineering* [online]. 2021, **750**, p. 495-507 [accessed 2023-09-19]. ISSN 1876-1119. Available from: https://doi.org/10.1007/978-981-16-0336-5_41/COVER
[15] BOUCHAIB, A., TALEB, R., MASSOUM, A., MEKHILEF, S. Geometric control of quadrotor UAVs using integral backstepping. *Indonesian Journal of Electrical Engineering and Computer Science* [online]. 2021, **22**(1), p. 53-61 [accessed 2023-09-21]. ISSN 2502-4760. Available from: https://doi.org/10.11591/IJEECS.V22.I1.PP53-61
[16] MOEINI, A., LYNCH, A. F., ZHAO, Q. A backstepping disturbance observer control for multirotor UAVs: theory and experiment. *International Journal of Control* [online]. 2022, **95**(9), p. 2364-2378 [accessed 2023-09-19]. ISSN 1366-5820. Available from: https://doi.org/10.1080/00207179.2021.1912393
[17] ARGENTIM, L. M., REZENDE, W. C., SANTOS, P. E., AGUIAR, R. A. PID, LQR and LQR-PID on a quadcopter platform. In: 2013 International Conference on Informatics, Electronics and Vision ICIEV 2013: proceedings [online]. IEEE. 2013. ISBN 978-1-4799-0397-9, eISBN 978-1-4799-0400-6. Available from: https://doi.org/10.1109/ICIEV.2013.6572698
[18] AHMAD, F., KUMAR, P., BHANDARI, A., PATIL, P. P. Simulation of the quadcopter dynamics with LQR based control. *Materials Today: Proceedings* [online]. 2020, **24**(2), p. 326-332. ISSN 2214-7853. Available from: https://doi.org/10.1016/j.matpr.2020.04.282
[19] ELTAYEB, A., RAHMAT, M. F., ELTOUM, M. A. M., IBRAHIM, M. H. S., BASRI, M. A. M. Trajectory tracking for the quadcopter UAV utilizing fuzzy PID control approach. In: 2020 International Conference on Computer, Control, Electrical, and Electronics Engineering, ICCCEEE 2020: proceedings [online]. IEEE. 2021. eISBN 978-1-7281-9111-9. Available from: https://doi.org/10.1109/ICCCEEE49695.2021.9429636
[20] TALHA, M., ASGHAR, F., ROHAN, A., RABAH, M., KIM, S. H. Fuzzy logic-based robust and autonomous safe landing for UAV quadcopter. *Arabian Journal for Science and Engineering* [online]. 2019, **44**(3), p. 2627-2639 [accessed 2023-09-19]. ISSN 2191-4281. Available from: https://doi.org/10.1007/S13369-018-3330-Z/METRICS
[21] BREESE, B., SCOTT, D., BARAWKAR, S., KUMAR, M. Fuzzy logic controller for force feedback control of quadcopter via tether. In: ASME 2020 Dynamic Systems and Control Conference DSCC 2020: proceedings [online] [accessed 2023-09-19]. 2021. Available from: https://doi.org/10.1115/DSCC2020-3275
[22] DARWITO, P. A., INDAYU, N. Adaptive neuro-fuzzy inference system based on sliding mode control for quadcopter trajectory tracking with the presence of external disturbance. *Journal of Intelligent Systems and Control* [online]. 2023, **2**(1), p. 33-46 [accessed 2023-09-19]. ISSN 2957-9805. Available from: https://doi.org/10.56578/JISC020104

[23] KORKMAZ, D., ACIKGOZ, H., USTUNDAG, M. Altitude and attitude control of a quadcopter based on neuro-fuzzy controller. *Lecture Notes in Electrical Engineering* [online]. 2022, **829**, p. 1009-1015 [accessed 2023-09-19]. ISSN 1876-1119. Available from: https://doi.org/10.1007/978-981-16-8129-5_154/COVER
[24] ABDOLAHI, Y., REZAEIZADEH, A. Black-box identification and iterative learning control for quadcopter. In: 2018 6th International Conference on Control Engineering and Information Technology CEIT 2018: proceedings [online]. IEEE. 2018. eISBN 978-1-5386-7641-7. Available from: https://doi.org/10.1109/CEIT.2018.8751795
[25] PIPATPAIBUL, P., OUYANG, P. R. Application of online iterative learning tracking control for quadrotor UAVs. *International Scholarly Research Notices* [online]. 2013, **2013**, 476153. ISSN 2356-7872. Available from: https://doi.org/10.5402/2013/476153
[26] BEHERA, L., KAR, I. *Intelligent systems and control: principles and applications*. New Delhi, India: Oxford University Press, 2010. ISBN 9780198063155.
[27] PEDRO, J. O., KALA, P. J. Nonlinear control of quadrotor UAV using Takagi-Sugeno fuzzy logic technique. In: 2015 10th Asian Control Conference ASCC: proceedings [online]. IEEE. 2015. eISBN 978-1-4799-7862-5. Available from: https://doi.org/10.1109/ASCC.2015.7244739
[28] NOSHADI, A., SHI, J., LEE, W. S., SHI, P., KALAM, A. Optimal PID-type fuzzy logic controller for a multi-input multi-output active magnetic bearing system. *Neural Computing and Applications* [online]. 2016, **27**(7), p. 2031-2046 [accessed 2024-01-17]. ISSN 0941-0643. Available from: https://doi.org/10.1007/S00521-015-1996-7/METRICS
[29] BOUABDALLAH, S. Design and control of quadrotors with applications to autonomous flying [online]. Lausanne, EPFL, 2007. Available from: https://doi.org/10.5075/epfl-thesis-3727
[30] SAUD, L. J., MOHAMMED, S. R. Performance evaluation of a PID and a fuzzy PID controllers designed for controlling a simulated quadcopter rotational dynamics model. *Journal of Engineering* [online]. 2017, **23**(7), p. 74-93 [accessed 2024-01-13]. ISSN 2520-3339. Available from: https://doi.org/10.31026/J.ENG.2017.07.05
[31] BRESCIANI, T. Modelling, identification and control of a quadrotor helicopter. MSc theses [online]. 2008 [accessed 2024-01-13]. ISSN 0280-5316. Available from: http://lup.lub.lu.se/student-papers/record/8847641
[32] MATTAVELLI, P., ROSSETTO, L., SPIAZZI, G., TENTI, P. General-purpose fuzzy controller for DC-DC converters. *IEEE Transactions on Power Electronics* [online]. 1997, **12**(1), p. 79-86 [accessed 2023-09-21]. ISSN 0885-8993. Available from: https://doi.org/10.1109/63.554172